Supporting Information

Development of neuron model based on DNAzyme regulation

Cong Chen [1], Ranfeng Wu[2] and Bin Wang [1,*]

[1] Key Laboratory of Advanced Design and Intelligent Computing, Dalian University, Ministry of Education, Dalian 116622, China; m17862859321@163.com(C.C.), wangbinpaper@gmail.com(B.W.)
[2] School of Computer Science and Technology, Dalian University of Technology, Dalian 116024, China;
* Correspondence: wangbinpaper@gmail.com(B.W.)

1 Weight unit 2

In order to fully realize the function of an artificial neuron in the experimental work, we verified the feasibility of the other two weight units.

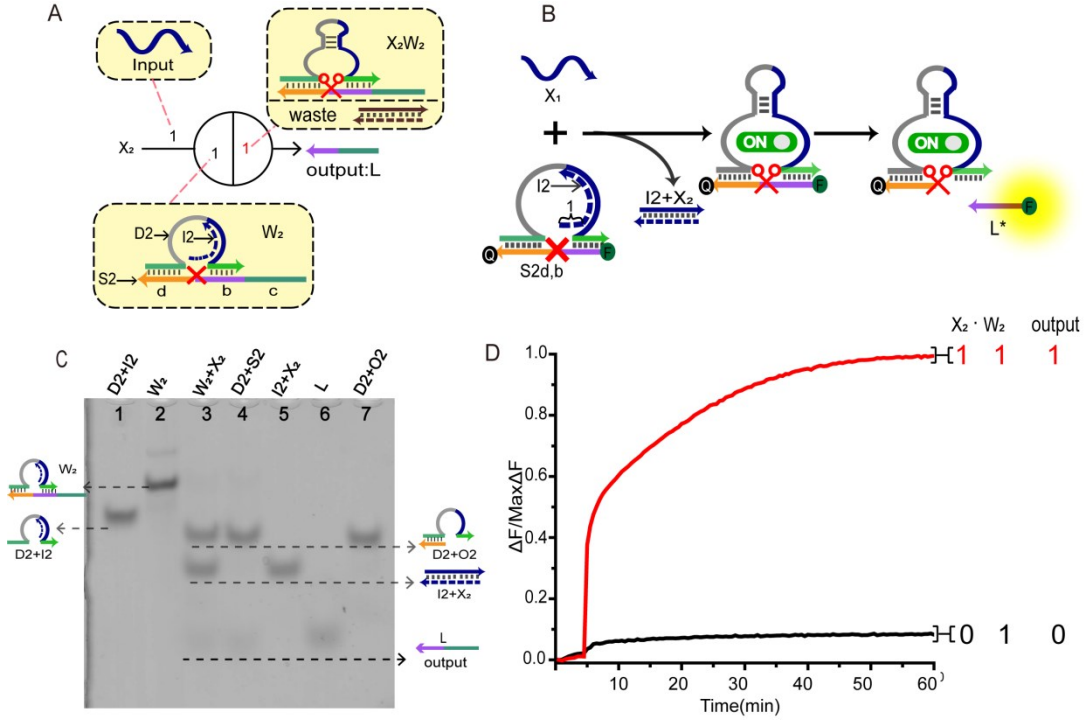

Figure S1. (A) Abstract diagram of the weight unit 2 motif and its DNA implementation. The black numbers indicate the initial relative concentration. Red numbers indicate relative product concentrations, and different colors indicate distinct DNA sequences. $S2_d$ is the left (3'-end) recognition domain of substrate strand 2(S2), while $S2_b$ is the right (5'-end) recognition domain of S2. **(B)** Illustration of the weight unit 2. The substrate strand sequence is $S2_{a,b}$, 5'-end fluorophore FAM and 3'-end quencher BHQ1 for fluorescent signal determination. **(C)** Native PAGE analysis of the weight unit 2. The strands and complex involved were labeled above the lane number. Lane 1, complex (D2+I2) consists of DNAzyme 2(D2) and inhibitor 2(I2); lane 2, weight unit 2(W_2) consisting of D2, I2 and S2; lane 3, products of W_2 triggered by input X_2; lane 4, products of D2 digestion; lane 5, complex ($I2+X_2$); lane 6, output strand L; Lane 7, complex (D2+O2). **(D)**Time-dependent fluorescence changes according to different inputs. The red curve reflects the reaction with the addition of X_2 and the black curve is the case with no input.

The reaction could be depicted in Figure S1 B. The cutting activity of D2 was inhibited because of the catalytic core of D2 hybridizes with the I2, while the substrate $S2_{d,b}$ could not be cut.The reaction could only be triggered after the addition of input signal X_2.The properties of W_2 was determined by native PAGE gel electrophoresis and fluorescence assay.

Figure S1 C shows PAGE analysis of W_2. Lane 2 indicated that the initial W_2 was present and stable in a single gel band. Lane 3, in the presence of input signal X_2, the W_2 band disappeared to produce three new bands (D2+O2), ($I2+X_2$) and L. Lane 4 was D2 cutting the S2 directly, resulting in two new bands (D2+O2) and L. It was proved that D2 restored the

activation of DNAzyme after adding the input signal. The PAGE gel experiment results prove the correctness of W_2.

Fluorescence measurements was also performed to detect the performance of W_2.The red curve indicated that the input signal X_2 was added, and a significant fluorescence increase can be observed. On the contrary, no remarkable increase of fluorescent signal could be observed in the black curve without the addition of input strand X_2. The results demonstrate the successful performance of W_2.

2 Weight unit 3

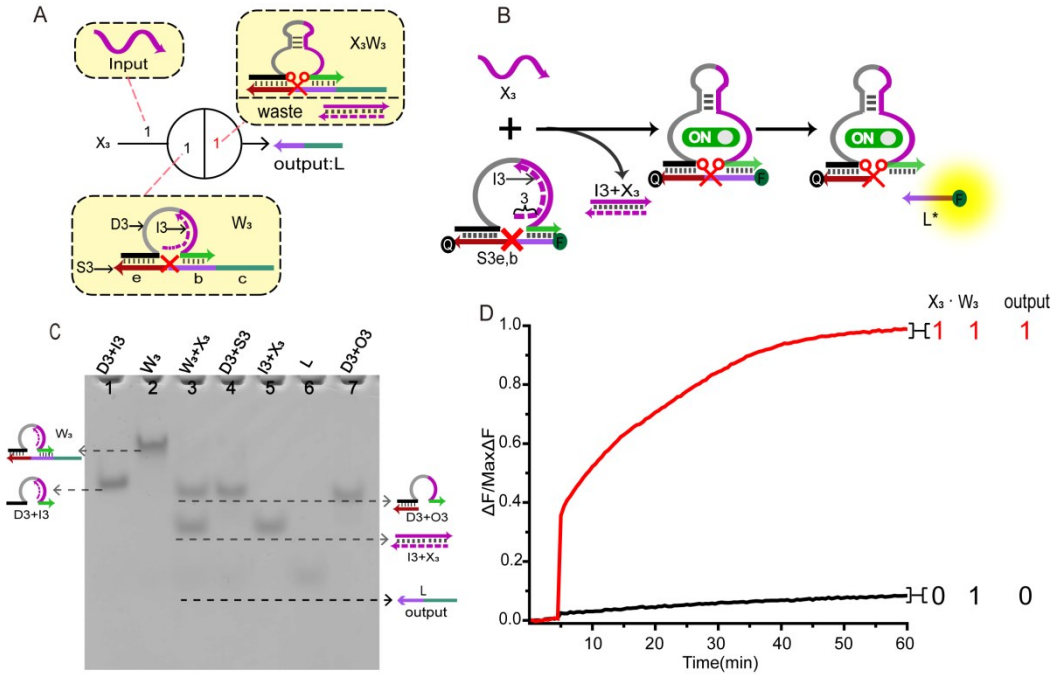

Figure S2. (A) Abstract diagram of the weight unit 3 motif and its DNA implementation. The black numbers indicate the initial relative concentration. Red numbers indicate relative product concentrations, and different colors indicate distinct DNA sequences. $S3_e$ is the left (3'-end) recognition domain of substrate strand 3(S3), while $S3_b$ is the right (5'-end) recognition domain of S3. **(B)** Illustration of the weight unit 3. The substrate strand sequence is $S3_{e,b}$, 5'-end fluorophore FAM and 3'-end quencher BHQ1 for fluorescent signal determination. **(C)** Native PAGE analysis of the weight unit 3. The strands and complex involved were labeled above the lane number. Lane 1, complex (D3+I3) consists of DNAzyme 3(D3) and inhibitor 3(I3); lane 2, weight unit 3(W_3) consists of D3, I3 and S3; lane 3, products of W_3 triggered by input X_3; lane 4, products of D3 digestion; lane 5, complex ($I3+X_3$); lane 6, product strand L; Lane 7, complex (D3+O3). **(D)**Time-dependent fluorescence changes according to different inputs. The red curve reflects the reaction with the addition of X_3 and the black curve is the case with no input.

The reaction could be depicted in Figure S2 B. The cutting activity of D3 was inhibited because of the catalytic core of D3 hybridizes with the I3, while the substrate $S3_{e,b}$ could not be cut. The reaction could only be triggered after the addition of input signal X_3. The

properties of W_3 was determined by native PAGE gel electrophoresis and fluorescence assay.

Figure S2 C shows PAGE analysis of W_3. Lane 2 indicated that the initial W_3 was present and stable in a single gel band. Lane 3, in the presence of input signal X_3, the W_3 band disappeared to produce three new bands (D3+O3), (I3+X_3) and L. Lane 4 was D3 cutting the S3 directly, resulting in two new bands (D3+O3) and L. It was proved that D3 restored the activation of DNAzyme after adding the input signal. The PAGE gel experiment results prove the correctness of W_3.

A fluorescence measurement was also performed to detect the performance of W_3.The red curve indicated that the input signal X_3 was added, and a significant fluorescence increase can be observed. On the contrary, no remarkable increase of fluorescent signal could be observed in the black curve without the addition of input strand X_3. The results demonstrate the successful performance of W_3.

3 Integration gate

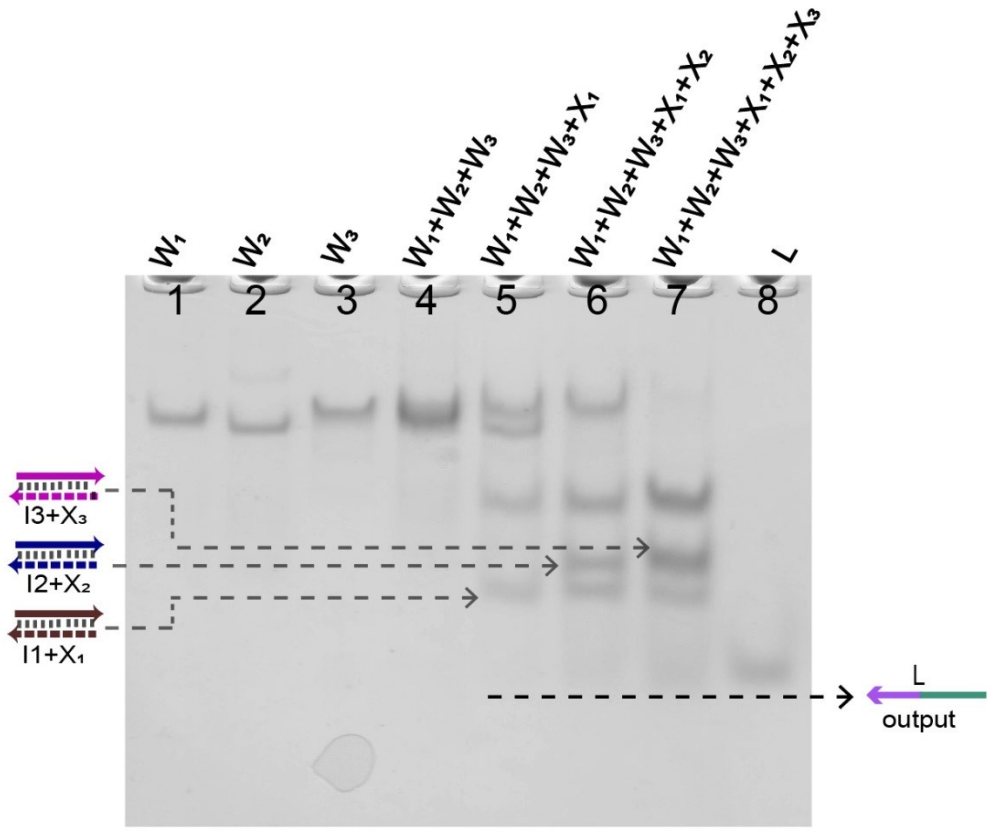

Figure S3. Native PAGE analysis of the integration gate. The strands and complex involved were labeled above the lane number. Lane 1, weighted unit 1 (W_1); lane 2, weighted unit 2 (W_2); lane 3, weighted unit 3 (W_3); Lane 4, weighted unit mixture (W_1+W_2+W_3); lane 5, X_1 was added to the weight unit mixture; lane 6, X_1 and X_2 were added to the weight unit mixture; lane 7, all signals were added to the weight unit mixture; lane 8, normalized product strand L.

In order to reflect the summation function of neurons in detail, we verify the logic function of the integration gate by adding different inputs. As shown in Figure S3, Lane 1 indicated that the initial W_1 was present and stable in a single gel band; Lane 2 indicated that

the initial W_2 was present and stable in a single gel band; Lane 3 indicated that the initial W_3 was present and stable in a single gel band. From lane 4 to lane 7, the added input signals were 0, X_1, X_1+X_2, X_1+X_2+X_3. It can be observed that W_1 band disappeared in lane 5, and a new gel band L was generated at the bottom. In lane 6, the W_1 and W_2 disappeared, and a new band strand L more obvious than lane 5 was observed. In lane 7, the W_1, W_2 and W_3 bands all disappeared, resulting in the darkest color of the band L. This was because with the number of input signals increased, the more strand displacement reaction occurred, making the DNAzyme exert its ability to cut the substrate strand.

4 Threshold gate

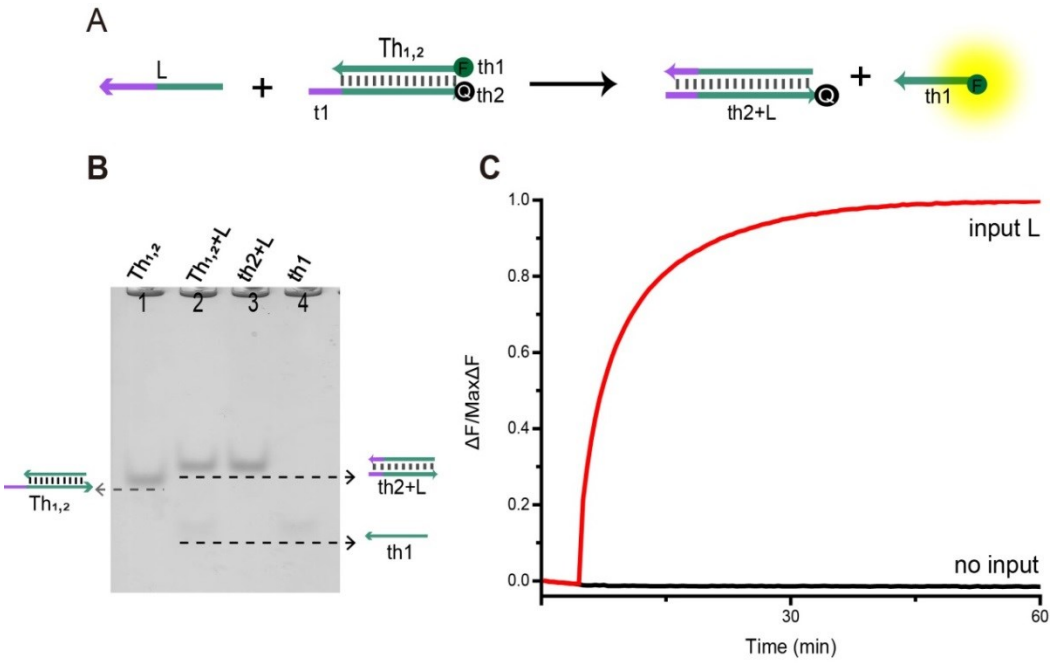

Figure S4. (A) Illustration of the Threshold gate. The top complementary strand th1 was labeled with the fluorophore FAM at the 5'-end and the bottom base strand th2 was labeled with the quencher BHQ1 at the 3'-end for fluorescent signal determination. **(B)** Native PAGE analysis of the Threshold gate. The strands and complex involved were labeled above the lane number. Lane 1, the $Th_{1,2}$(th1+th2) in the Threshold gate; Lane 2, products of Threshold gate triggered by input L([Th1, 2]:[L]=1:1); Lane 3, the product (th2 +L); Lane 4, the product th1. **(C)** The fluorescence of the Threshold gate. The red curve reflects the reaction with the addition of L and the black curve is the case with no input.

Figure S4 A describes the reaction process of the Threshold gate. The input signal strand L performed strand displacement reaction through the t1 to generate a stable double-stranded complex. Native PAGE analysis of the Threshold gate as shown in Figure S4 B. Lane 1 was the location of the $Th_{1,2}$ in the Threshold gate. When adding input signal strand L in lane 2, the band $Th_{1,2}$ disappear to produce two new gel bands (th2+L) and th1. A fluorescence assay was also performed to detect the performance of the Threshold gate (Figure S4 C). The red curve indicated that the input signal L was added and a significant fluorescence increase can be observed. On the contrary, no remarkable increase of

fluorescence signal could be observed in black curve without the addition of input strand L.

5 Reporter gate

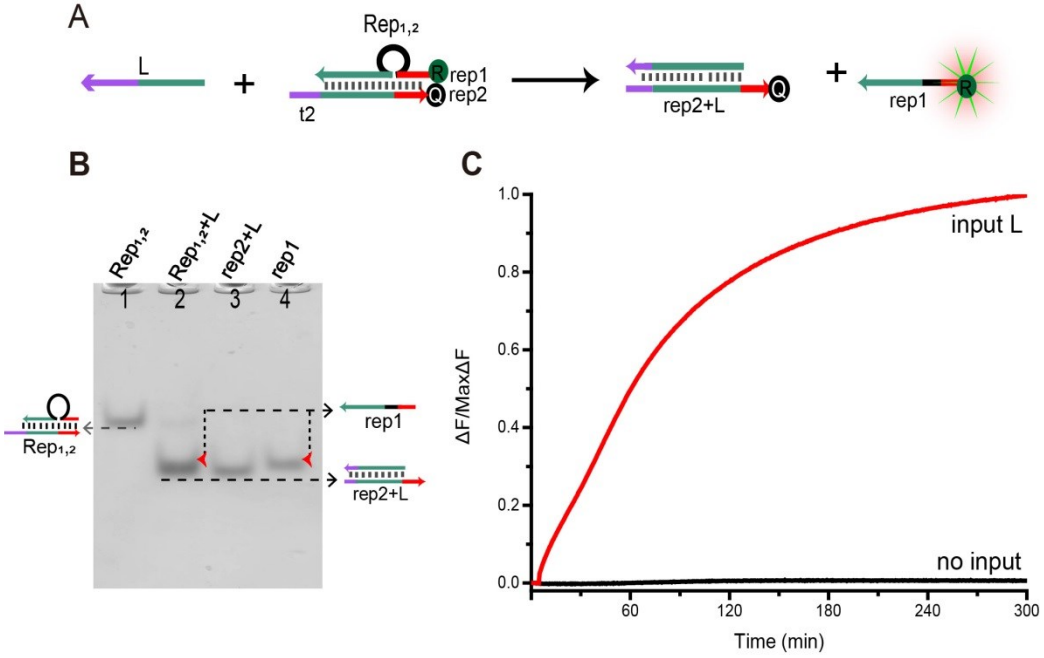

Figure S5. (A) Illustration of the Reporter gate. The strand rep2 3'-end marked quencher BHQ2, strand rep1 5'-end marked fluorophore ROX for fluorescence signal determination. **(B)** Native PAGE analysis of the Reporter gate. The strands and complex involved were labeled above the lane number. Lane 1, the $Rep_{1,2}$(rep1+rep2) in the Reporter gate; Lane 2, products of Reporter gate triggered by input L([Rep1,2]:[L]=1:1); Lane 3, the product (rep2+L); Lane 4, the product rep1. **(C)** The fluorescence of the Reporter gate. The red curve reflects the reaction with the addition of L and black curve is the case with no input.

Figure S5 A describes the reaction process of the Reporter gate. The input signal strand L performed strand displacement reaction through the t2 to generate a double-stranded complex. Native PAGE analysis of the Reporter gate as shown in Figure S5 B. Lane 1 was the location of the $Rep_{1,2}$ in the Reporter gate. When adding input signal strand L in lane 2, the band $Rep_{1,2}$ disappear to produce two new gel bands (rep2+L) and rep1. Fluorescence measurements were also performed to detect the performance of the Reporter gate (Figure S5 C). The red curve indicated that the input signal L was added and a significant fluorescence increase can be observed. No input signal was added to the black curve, so no remarkable increase of fluorescence signal could be observed.

6 Reporter gate optimization

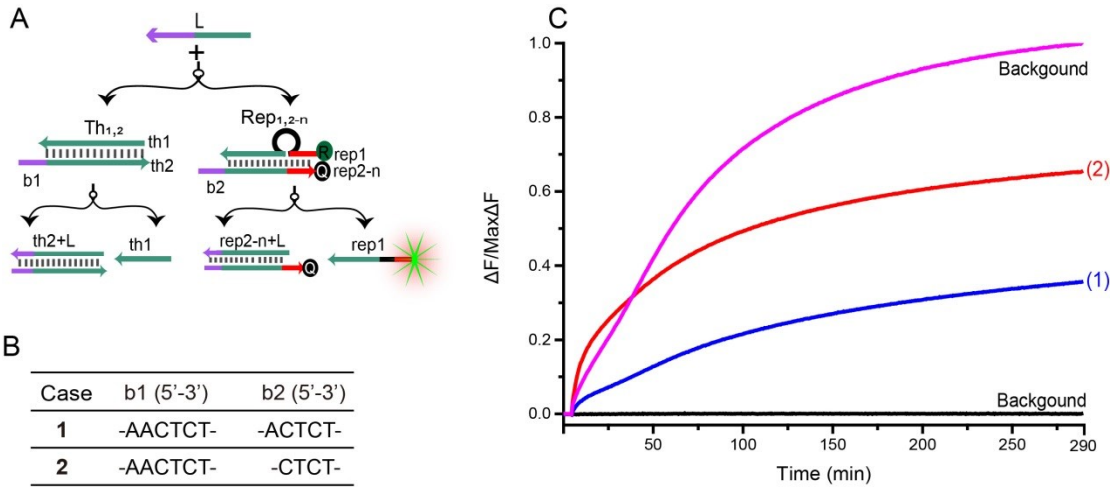

B

Case	b1 (5'-3')	b2 (5'-3')
1	-AACTCT-	-ACTCT-
2	-AACTCT-	-CTCT-

Figure S6. (A) Illustration of the Thresholding gate. The $Rep_{1,2}$ consists of a base strand rep2 and a top strand rep1. At the top of the strand rep1 5'-end labeled fluorophore ROX, base strand rep2 3'-end labeled quencher BHQ2 for fluorescence signal determination, rep2-n (n=1,2) represents the sequence in figure S6 B(rep2 has the same sequence as rep2-2). **(B)** The base sequence table of the toehold domain of the Threshold gate and the Reporter gate. **(C)** The fluorescence of the Reporter gate optimization. The ratio of $[Th_{1,2}]$, $[Rep_{1,2\text{-}n}]$ and [L] was 1:1:1.($[Th_{1,2}]$:$[Rep_{1,2\text{-}n}]$:[L]=1:1:1). The lowest background signal when the Report gate was completely quenched(black curve).The maximum fluorescence achieved by the complete reaction of the Reporter gate indicated the highest background signal(pink curve). The optimal number of toehold domain was selected by comparing with the background signal. Curve (1) represent the toehold sequence in Case 1, and curve (2) represent the toehold sequence in Case 2.

In order to obtain the optimal thresholding processing performance, the input signal strand L should react with the Threshold gate first. In the case that the Threshold gate toehold domain has 6 bases, we adjust the number of bases in the toehold domain of the Reporter gate to ensure that L takes precedence with the Threshold gate reaction. The strategy of reducing leakage by reducing the number of bases in the toehold domain of the Reporter gate was feasible, but considering the rate of biochemical reaction, we set b2 to have at least 4 bases. Equal proportions of $[Th_{1,2}]$, $[Rep_{1,2\text{-}n}]$ and [L] were added to the solution to observe their fluorescence changes. As shown in Figure S6 C,Curve (2) indicated the leakage situation of b2 has 5 bases; Curve (1) indicated the leakage situation of b1 has 4 bases. It can be observed that the optimal thresholding processing performance can be obtained when the b1 has 6 bases and b2 has 4 bases.

7 An artificial DNA neuron model

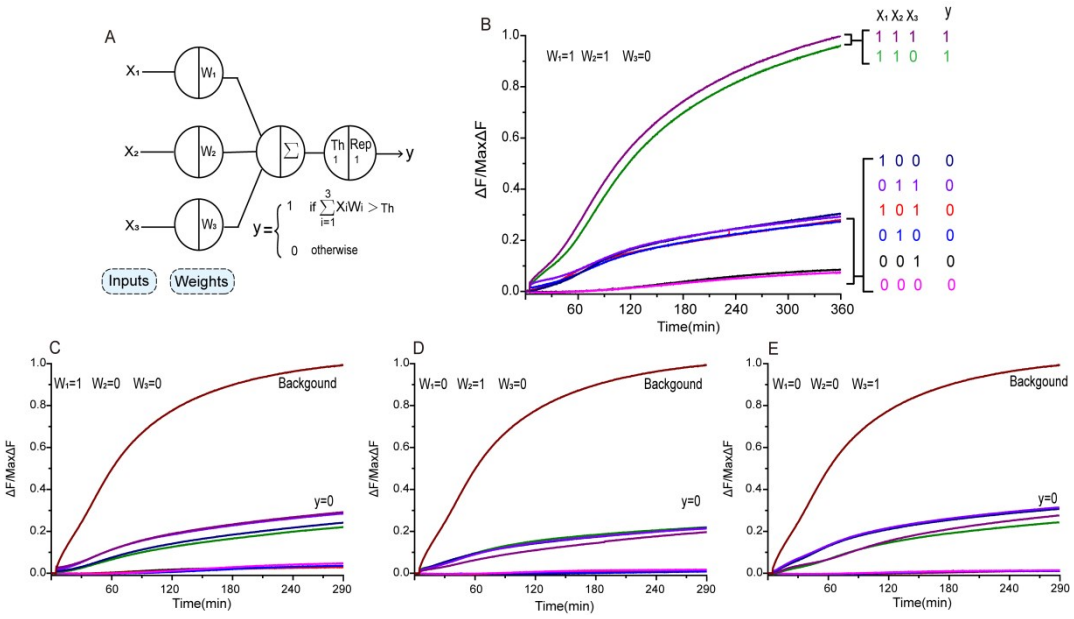

Figure S7. (A) Demonstration of a 3-input 1-output linear threshold gate. Each value was represented by a relative concentration. It calculates the sum of the 3-input($\sum_{i=1}^{3} X_i \cdot W_i$). **(B)** Fluorescence detection with W_1=1, W_2=1, W_3=0. **(C)** Fluorescence detection with W_1=1, W_2=0, W_3=0. The maximum fluorescence achieved by the complete reaction of the Reporter gate indicated the highest background signal (the top curve). **(D)** Fluorescence detection with W_1=0, W_2=1, W_3=0. The maximum fluorescence achieved by the complete reaction of the Reporter gate indicated the highest background signal (the top curve). **(E)** Fluorescence detection with W_1=0, W_2=0, W_3=1. The maximum fluorescence achieved by the complete reaction of the Reporter gate indicated the highest background signal (the top curve). In fluorescence measurements the standard concentration was 1×=0.2 uM. Input strands X_1, X_2 and X_3 were then added with relative concentrations of 0×or 1×.

The output values were inferred by fluorescence signals normalized to the maximum completion level. When weight W_1 =1, W_2 =1 and W_3 =0, the output results were shown in Figure S7 B; When weight W_1 =1, W_2 =0 and W_3 =0, the output results were shown in Figure S7 C; When weight W_1 =0, W_2 =1 and W_3 =0, the output results were shown in Figure S7 D; When weight W_1 =0, W_2 =0 and W_3 =1, the output results were shown in Figure S7 E. Both weight conditions achieved the correct ON or OFF state with the complete 8 sets of inputs.

8 Optimization of weight unit and threshold gate

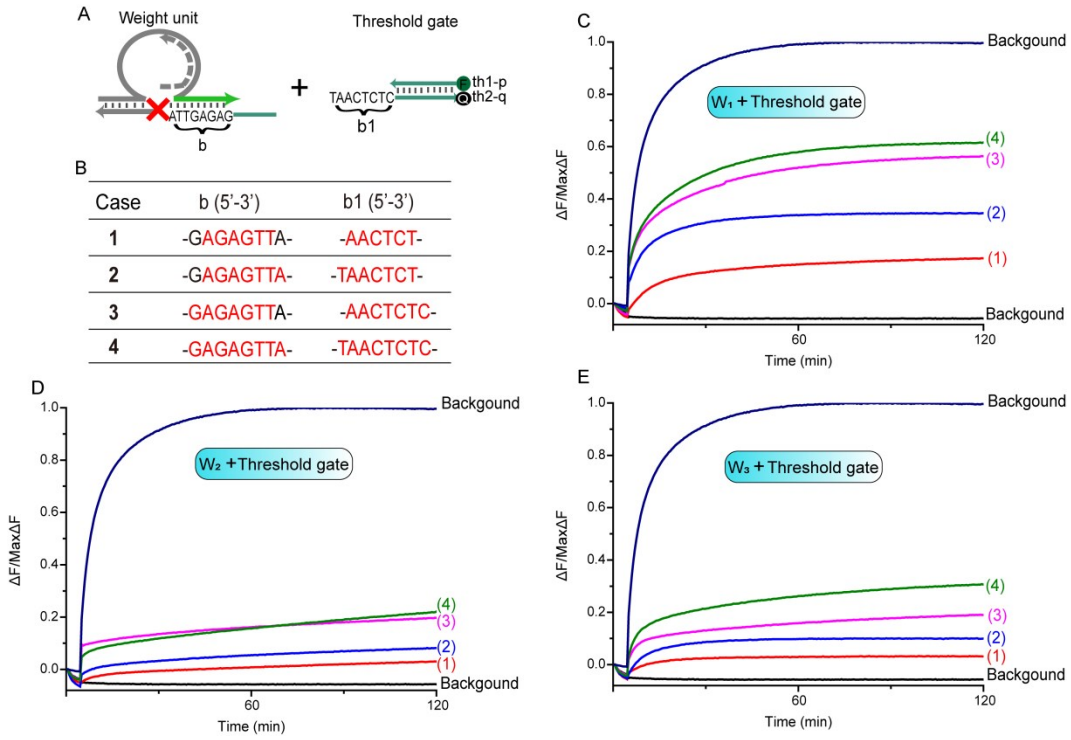

Figure S8. (A) Illustration of the weight unit and Threshold gate leakage. The $Th_{1\text{-}p,2\text{-}q}$ in the Threshold gate consists of a base strand th2-q(q=1,2) and a top strand th1-p(p=1,2). At the top of the strand 5'-end labeled fluorophore FAM, base strand 3'-end labeled quencher BHQ1 for fluorescence signal determination (th1-1 has the same sequence as th1, th2-1 has the same sequence as th2). **(B)** The base sequence table of the toehold domain of the weight unit and the Threshold gate. **(C)** The fluorescence of the weight unit 1 and the Threshold gate. **(D)** The fluorescence of the weight unit 2 and the Threshold gate. **(E)** The fluorescence of the weight unit 3 and the Threshold gate. The lowest background signal indicated the Threshold gate was completely quenched(black curve).The maximum fluorescence achieved by the complete reaction of the Threshold gate indicated the highest background signal(the top curve). The optimal number of toehold domain in Threshold gate was selected by comparing with the background signal.

In order to obtain the optimal performance of the neuron model, we optimized the Threshold gate. Leakage was unavoidable in the molecular system, so we reduce the system leakage by adjusting the position of the complementary base sequence of the Threshold gate in the weight unit. The domain of b where the normalized product L can be used to trigger the downstream reaction has 8 bases. Due to the insufficient binding ability of the DNAzyme binding arm to the substrate, we suspect that there was a certain leakage between the weight unit and the Threshold gate. By adjusting the sequence of b1, the leakage in the experiment was optimized, and the results were verified by fluorescence experiments. The leakage reaction between weight unit 1 and Threshold gates with different toehold as shown in Figure S8 C. Curves (1) - (4) correspond to Case 1-4 in Figure S8 B. The fluorescence results of weight unit 2 and weight unit 3 were shown in Figure S8 D and S8 E respectively. Curve

labels correspond to the b1 sequence in Figure S8 B. By fluorescence detection results, it can be observed that curve (1) in each fluorescence figure has the least fluorescence growth, so we used the base sequence shown in Case 1 as the toehold domain of the Threshold gate.

9 Voting machine

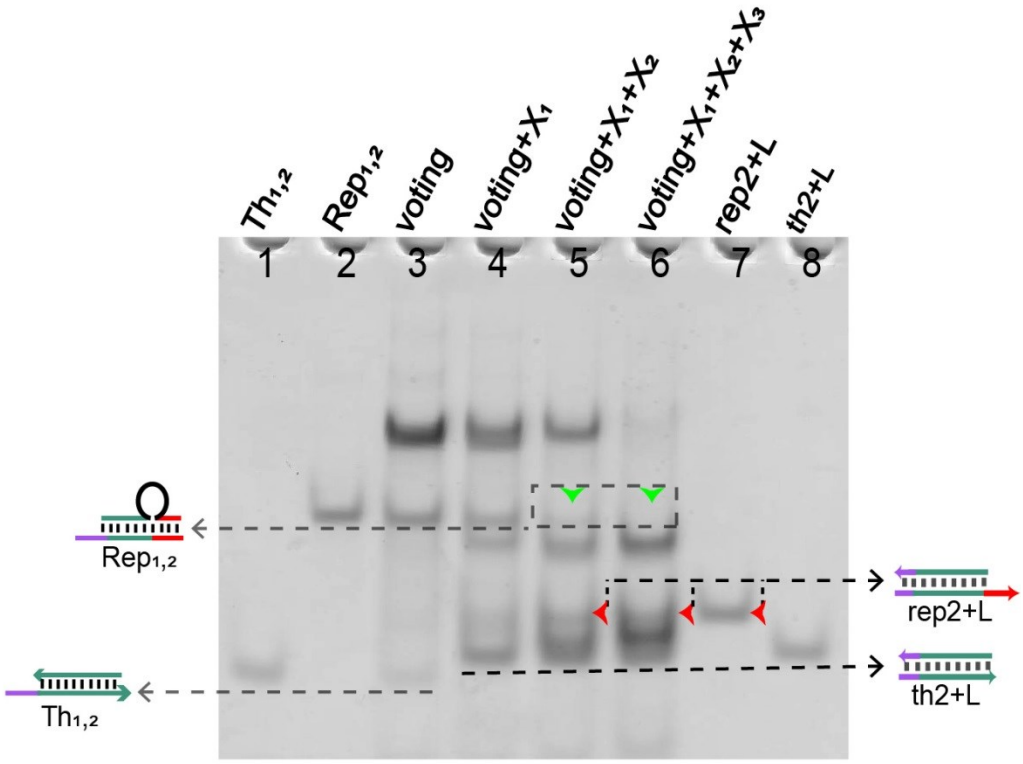

Figure S9. Native PAGE analysis of the voting circuit. The strands and complex involved were labeled above the lane number. The voting system consisted of [W_1], [W_2], [W_3], [$Th_{1,2}$], [$Rep_{1,2}$], and their proportion of 1:1:1:1:1. Different inputs were added to validate the voting result. Lane 1, the $Th_{1,2}$(th1+th2); Lane 2, the $Rep_{1,2}$(rep1+rep2); lane 3, the components required for voting system; lane 4,the signal X_1 was added to the voting system; lane 5, the signal X_1 and X_2 were added to the voting system; lane 6, all input signals X_1, X_2 and X_3 were added to the voting system; lane 7, the product of the Reporter gate(rep2+L); lane 8, the product of the Threshold gate(th2+L).

As shown in Figure S9, lane 3 was the voting system in the initial state, and the two bands $Rep_{1,2}$ and $Th_{1,2}$ can be clearly observed. Lane 4 was added an input signal X_1, which by rule was invalid if only one voter "agree", so the band $Rep_{1,2}$ still existed in lane 4. The input signals X_1+X_2, X_1+X_2+X_3 were also added to lanes 5 to 6 respectively. In these two lanes, the gel band $Rep_{1,2}$ disappeared(the green arrow shows the position) and a new band (rep2+L) was generated(the red arrow shows the position).

10 DNA sequences

Name	Sequences (from 5′to 3′)	Length (n.t.)
D1	GAGCGATCTAGCAGCGATATCACGCCTCGTCTGGCGTGATCACCCATGTTAACTCTC	57
I1	AATCGATCATGGGTGATCACGCCA	24
S1	TTGACGAGTCCACCAGAGAGTTAT/rA/GGCTAGATCGCTC	39
X1	AGGCGTGATCACCCATGATCGATT	24
O1	GGCTAGATCGCTC	13
S1a,b	GAGAGTTAT/rA/GGCTAGATCGCTC	24
D2	TAGTGTATGTTCAGCGATGACTCGTCTTGTTGACGAGTCCACCCATGTTAACTCTC	56
I2	AGATATTCATGGGTGGACTCGTCAA	25
S2	TTGACGAGTCCACCAGAGAGTTAT/rA/GGAACATACACTA	39
X2	TTGACGAGTCCACCCATGAATATCT	25
O2	GGAACATACACTA	13
S2d,b	GAGAGTTAT/rA/GGAACATACACTA	24
D3	TGTCATTCGTTCAGCGATCTCAGGTGTGTATCACCTGAGCACCCATGTTAACTCTC	56
I3	CATATCTCATGGGTGCTCAGGTGATA	26
S3	TTGACGAGTCCACCAGAGAGTTAT/rA/GGAACGAATGACA	39
X3	GTATCACCTGAGCACCCATGAGATATG	27
O3	GGAACGAATGACA	13
S3e,b	GAGAGTTAT/rA/GGAACGAATGACA	24
L	TTGACGAGTCCACCAGAGAGTTATA	25
L*	GAGAGTTAT/rA/	10
th1	CTTGACGAGTCCACCAG	17
th1-2	CTTGACGAGTCCACCA	16
th2	AACTCTCTGGTGGACTCGTCAAG	23
th2-2	TAACTCTCTGGTGGACTCGTCAAG	24
rep1	TAGAGATTGTACCCACGGCAAGGCCTAGCGACTGACGAGTCCACCAG	47
rep2	CTCTCTGGTGGACTCGTCAATCTCTATTTTT	31
rep2-1	ACTCTCTGGTGGACTCGTCAATCTCTATTTTT	32

Table S1. DNA sequences

All of the sequences used in this work were designed using Nupack[1–3].

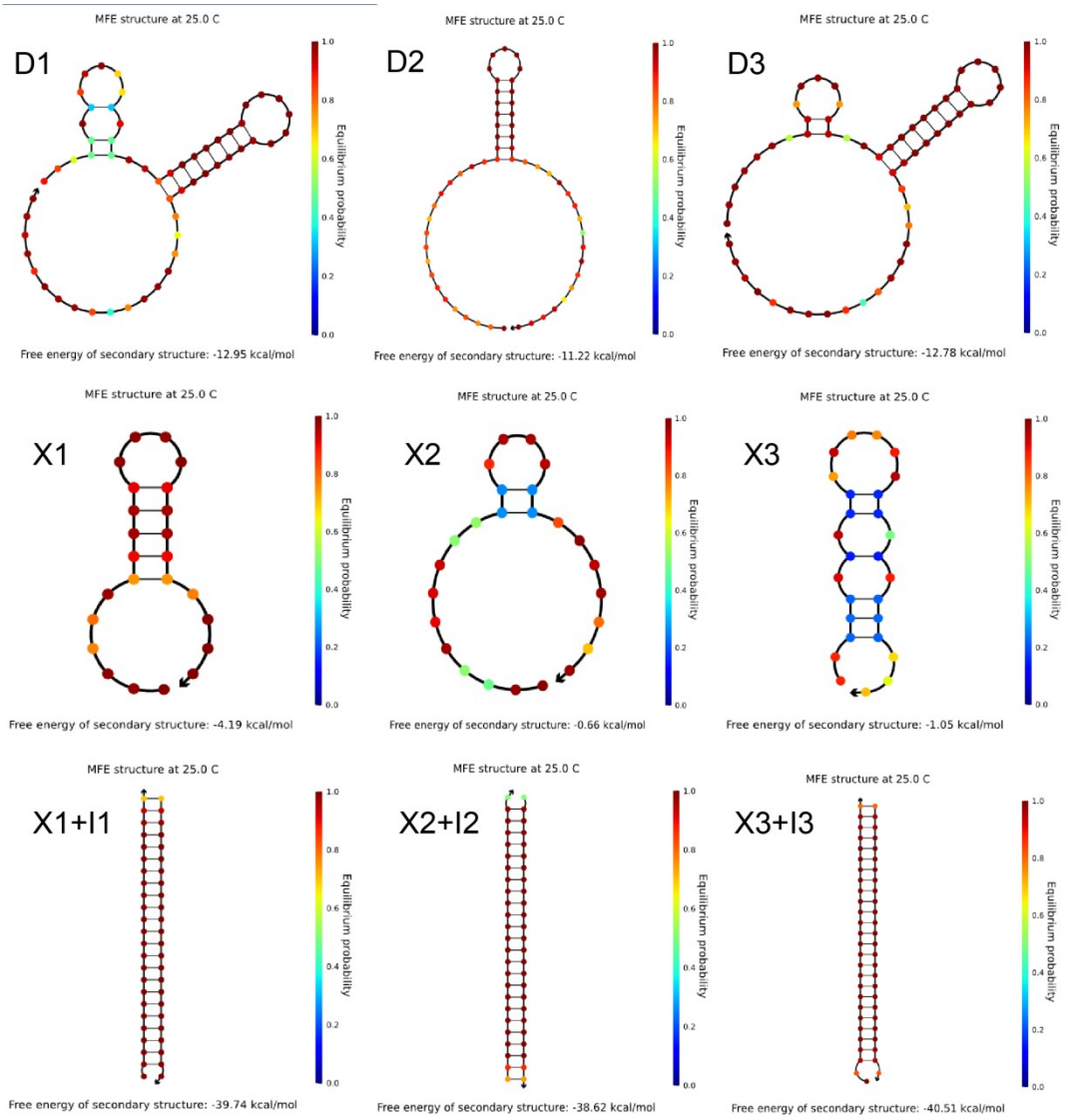

Figure S10. Nupack simulations for partial DNA sequences in table S1.

11 References

1 B. R. Wolfe, N. J. Porubsky, J. N. Zadeh, R. M. Dirks and N. A. Pierce, *J. Am. Chem. Soc.*, 2017, **139**, 3134–3144.

2 J. N. Zadeh, C. D. Steenberg, J. S. Bois, B. R. Wolfe, M. B. Pierce, A. R. Khan, R. M. Dirks and N. A. Pierce, *J. Comput. Chem.*, 2011, **32**, 170–173.

3 B. R. Wolfe and N. A. Pierce, *ACS Synth. Biol.*, 2015, **4**, 1086–1100.